Nat. Volatiles & Essent. Oils, 2021; 8(6): 5017-5037

NVEO
Natural Volatiles &
Essential Oils

Preparation, Characterization And Evaluation Of Chitosan Nanobubbles For The Targeted Delivery Of Ibrutinib

Muralikrishna Ponnaganti[1] , Ancha Kishore Babu[2]

[1]Shridhar University, Chirava- Pilani road, Pilani-333031, Rajasthan, India.

[2]Raffles University, Japanese zone, NH 8, Neemrana-301020, Rajasthan, India.

ABSTRACT

In present research, we presented a new approach for formulating nanosized, Ibrutinib bubbles by incorporation into chitosan shelled nanobubbles. The effect of L-α- Phosphatidylcholine (A), concentration of chitosan (B) and concentration of palmitic acid (C), on the particle size and polydispersity index of nanobubbles as studied by 3^3 Box-Behnken design. About 17 experiments were randomly arranged by Design Expert® software and statistically analyzed by multiple regression analysis .the optimized formulation obtained using numerical optimization technique by setting restrictions on the response parameters. The three optimized (B1-B3) formulations were evaluated. The results reveal that the superficial morphology and core-shell structure of nanobubbles was in the size range of 150-200 nm. The nanobubble formulations were able to load ibrutinib with an encapsulation efficiency of 82.58 % and loading capacity of 17%. In vitro release profile of ibrutinib from nanobubbles show that amount of drug released from nanobubbles was significantly higher(93.52%) than that from the ibrutinib suspension within 24h. according to fluorescent intensity data generated from HepG2 cells, mean fluorescence intensity of 6.12 in HepG2 cells, which is 1.5 times higher than that treated with Ibrutinib Nanobubbles without ultrasound. The In-vitro cytotoxicity study indicated that ultrasound assisted nanobubbles can effectively release in the cells with high sensitivity.

The results have shown that the nanobubbles were better apposite for contrast enhanced tumor imaging and subsequent therapeutic delivery.

Keywords: Ibrutinib, B cell cancer, chitosan shelled nanobubbles, perfluoropentane, Box-Behnken design (BBD)

INTRODUCTION

Many nanoparticles drug delivery systems have been utilized in cancer healing with rapid development of cancer-targeted nanotech [1]. In spite of intense nanomedicine research, majority of applications could not make till clinical practice. To posses' theaurapatic effect, drug nano-carriers should penetrate various biological barriers post intravenous injection to reach the targeted site and become intracellular. Researchers have explored various controlled delivery using nanocarriers. These constraints can be

appreciably enhanced if an external physical mechanism is applied, such as an electric, electromagnetic or mechanical device [2].

Liposome's, micelle and nanobubble formulations were developed for US-triggered drug dissolution outside bloodstream to overcome this limitation. Nanobubbles are sphere shaped core/shell structures packed by gases, such as perfluorocarbons, that are nanometricin range, and are designed toenhance stability and advance the bio-distribution of drug to effected region. Their structure consists of a core that is stabilized by alipid, polymer, or by an albumin shell. [3].

Chitosan based nanobubbles are attracting attention owing to its natural origin, quality, biodegradable and biocompatible nature, low immunogenicity and antibacterial property.A N-deacetylated derivative of chitin, chitosan is one of the most abundant substances on the planet.

Consequently, Chitosan serves as a more effective anticancer drug carrier because of its direct and indirect antitumor effects [4].

Ibrutinib, is a small molecule drug that inhibits B-cell proliferation and survival by irreversibly binding the protein Bruton's tyrosine kinase (BTK). Blocking BTK inhibits the B-cell receptor pathway, which is often aberrantly active in B cell cancers. Our study was designed to develop ibrutinib loaded chitosan nanoparticles with the desired size and physicochemical properties to improve treatment efficacy.

Nowadays, various experimental designs are useful in developing a formulation requiring less experimentation and providing estimates of the relative significance of different variables. In recent times, the application of a statistical experimental design to pharmaceutical formulation has been demonstrated to be efficient at acquiring the necessary information to understand the relationship between independent and dependent variables in a formulation. The response surface methodology (RSM) is useful in simultaneously analyzing process variables when variable interactions are very complicated. Many studies have demonstrated the value of RSM for establishing the optimal formulation in various drug delivery systems. This study used the Box-Behnken design, an RSM design, because it requires fewer runs in a 3-factor experimental design than all other RSM designs, and is particularly useful when extreme treatment combinations need to be avoided. The aim of this research was to evaluate the main and interaction effect of compositional variation and to optimize the ibrutinib -loaded nanobubbles formulation using BBD.

MATERIALS AND METHODS

Ibrutinib is a gift from Dr. Reddy's Lab, Hyderabad, India while Chitosan and other excipients obtained from Sigma-Aldrich, India. Perfluoropentane purchased from Pharm affiliates, Haryana, India.

Preparation of chitosan shelled nanobubbles

Nanobubbles were prepared using perfluoropentane for the inner core and chitosan (~190,000 Da, degree of deacetylation 75%–85%) for the shell.

Nanobubbles were prepared as per the method reported elsewhere with slight modification. L-α-Phosphatidylcholine and palmitic acid were dissolved in 3 ml of ethylalcohol and added to 5 ml perfluoropentane under stirring at room temperature to form a pre-emulsion. This emulsion was suitably diluted with ultrapure water and homogenized using a high shear homogenizer (T 25 digital ULTRA-TURRAX®) for 5 minutes at 12000 rpm in an ice bath. Finally, the chitosan solution (pH 5.0) was transferred drop wise under mild magnetic stirring. The formed nanobubbles formulation was purified

by ultra-filtration, using a TCF2 instrument (Millipore) with a membrane cut-off diameter of 100000. Finally, a PluronicF68 solution (0.01% v/v) was added to nanobubbles formulation as a stabilizing layer. The contents subjected to incubation for 30 min followed characterization.[6]

Preparation of ibrutinib loaded chitosan nanobubbles

Ibrutinib (100 mg) was mixed with perfluoropentane core dissolved in ethyl alcohol as co-solvent, to facilitate drug release. L-α- Phosphatidylcholine and palmitic acid were dissolved in ethanol and mixed with ibrutinib-perfluoropentane solution to form a pre-emulsion. The procedure was similar to that adopted for chitosan shelled nanobubbles.

Optimization of critical parameters using design of experiments

From the preliminary studies, it was found that concentration of L-α- Phosphatidylcholine (A), concentration of chitosan (B) and concentration of palmitic acid (C), had a noteworthy impact on the particle size and polydispersity index of nanobubbles. Therefore, BBD was employed to determine influence of factors affecting particle size, and polydispersity index.

The range and levels of every variable was identified based on the results of preliminary experiments (Table 1). As described by the BBD model, 17 experiments were randomly arranged by Design Expert® software. The experimental conditions for all the trials are presented in table 2.

Data analysis

The obtained results were subject to statistical analysis. The relationship between the variables can be described by using various models. Numerous statistical parameters like, model p value, p value of lack of fit, Regression coefficient (R^2), Adjusted R^2 and Coefficient of Variation were considered to select a suitable best fitting model. Usually, the model terms with p value greater 0.005 can be considered as insignificant and can be eliminated from the model. Each response parameter can be evaluated by quadratic model using multiple regression analysis as shown in equation 1.

$$Y = A_0 + A_1 X_1 + A_2 X_2 + A_3 X_3 + A_4 X_1^2 + A_5 X_2^2 + A_6 X_3^2 + A_7 X_1 X_2 + A_8 X_1 X_3 + A_9 X_2 X_3 \quad (1)$$

Where, Y – Response parameter

A_0 – Intercept

A_1– A_9 – regression coefficients

X_1, X_2 and X_3 – Main influencing factors

X_1X_2 – Interactive effect

X_1^2, X_2^2, X_3^2 – Quadratic effect

The independent variables which do not contribute to the regression equation will be deleted one at a time by backward elimination procedure. The 3D response surface plots (3D RSP) show the functional association among the selected response parameter and two independent variables. Perturbation (PP) and contour plots (CP) also can be used to visualize the influence of independent variables on response parameters.

Optimization

The optimal points for the independent variables were attained using numerical optimization technique by setting restrictions on the response parameters and influencing factors. The nano formulation was prepared in triplicate under optimal conditions to verify the validity optimization technique.

Table 1: BBD

Factors			**Levels**		
Variable		Units	Low	Intermediate	High
A	Conc. of L-α-Phosphatidylcholine	w/v	1	1.5	2
B	Conc. of Chitosan	w/v	1	2	3
C	Conc. of palmitic acid	w/v	0.5	1	1.5
Responses			**Goal**		
Y1	PLS	nm	Decrease		
Y2	PI	-	Decrease		

Characterization of nanobubbles formulation

Determination of PLS, PI and zeta potential (ZEP) [7]

The PLS and PI were analyzed by measurement of random change in intensity of light scattered from the nanoliposomal dispersion using Malvern particle size analyser (Master sizer 2000). Zeta potential of nanoliposomes was measured in an additional gold-plated electrode containing U shape cell at a count rate of 250 particles/second at 25°C. All the measurements were collected for three times.

Transmission electron microscopy (TEM)

JEOL JEM-2000FX TEM was employed to check the morphology and size of nanobubbles. One drop of aqueous solution of phosphotungstic acid was added to the diluted sample of formulation for staining before observation under TEM. [8]

Table 2: Observed responses of trial experiments as per BBD

Expt	**A (w/v)**	**B (w/v)**	**C (w/v)**	**PLS (nm)**	**PI**
1	1.5	2	1	398.83	0.26

2	1.5	3	1.5	198.12	0.16
3	1	1	1	322.72	0.32
4	1	2	0.5	416.42	0.51
5	1.5	2	1	394.16	0.27
6	1	3	1	246.72	0.29
7	2	3	1	252.78	0.28
8	1	2	1.5	345.72	0.2
9	2	2	1.5	368.34	0.26
10	2	1	1	326.18	0.32
11	1.5	2	1	400.12	0.27
12	1.5	3	0.5	272.46	0.44
13	1.5	1	1.5	293.12	0.22
14	1.5	2	1	399.12	0.25
15	2	2	0.5	402.82	0.44
16	1.5	1	0.5	322.42	0.43
17	1.5	2	1	396.44	0.26

Encapsulation efficiency (ETE) and loading capacity (DLC) [9]

Ibrutinib formulation (5 ml ≈ 1 mg of drug) was placed into dialysis bag (MWCO 12000-14000 da) and placed in 100 ml pH 7.4 phosphate buffer. 1M sodium thiocyanate was added to the dialysis medium. The experiment was conducted at a temperature of 37 °C and stirring speed of 100 rpm. 2 ml of the sample was withdrawn from the dialysis media after 60 min to measure amount of unbound drug. The formulation that remained in the dialysis bag was dissolved in a mixture of water and organic solvent (Methanol), to extract bound drug from the formulation. The concentration of both bound drug and unbound drug were measured by stability indicating HPLC method. The percent encapsulation efficiency was estimated as per the following equations:

$$Encapsulation\ efficiency\ = \frac{(Total\ amount\ of\ ibrutinib - Free\ ibrutinib)}{Total\ amount\ of\ ibrutinib}$$

$$Loading\ capacity\ = \frac{(Total\ amount\ of\ ibrutinib - Free\ ibrutinib)}{Weight\ of\ nanobubbles\ formulation}$$

Viscosity and refractive index of nanobubbles

The values determined at 25 °C using a capillary viscometer by abbe's refractometer.

Differential scanning calorimetry

The analysis carried out on PerkinElmer STA 8000 Thermal Analyzer at heating rate of 10 degrees Celsius/minute in the 30-400 degree temperature range. As a reference standard, an empty aluminum

sample pan (Perkin-Elmer) was used. Under nitrogen purge, we analyzed samples of 5 mg in triplicate. We made triple runs for each sample.

In vitro release (IVR) [10]

By the dialysis bag technique at 37 °C, the IVR data of ibrutinib from the nanobubbles was measured both in presence and absence of ultrasound. The release data recorded upto 24 h by taking out 1 ml of the receiving phase at fixed time point and replacing the liquid with fresh phosphate buffer. The IVR was also measured after ultrasound application (frequency 2.5 ± 0.1 MHz, insonation time = 1 min). According to previous reports, the drug release was measured for 24 hours after the nanobubbles had been inducted into the dialysis bag. All the samples were spectrophotometrically evaluated to determine the drug amount.

Ultrasound stability of ibrutinib nanobubbles [11]

Ibrutinib loaded nanobubbles were exposed to an ultrasound stimulus of oscillation frequency 2.5 ± 0.2 MHz and an average acoustic pressure distribution value of 2.5 ± 0.2 MPa, nominal frequency 50 Hz, and nominal power 30W. Formulations were evaluated before and after ultrasound exposure for 30s, 1, 2, 3, 4 and 5 min at 37 °C, following 10 min to rest, by morphological analysis using optical microscopy to evaluate the integrity of nanobubbles structure.

Evaluation of stability of ibrutinib nanobubbles [11]

The stability of ibrutinib nanobubbles was evaluated at different temperatures (4 °C, 25 °C and 40 °C) for 1 month. The content of ibrutinib, encapsulation efficiency and the average particle size of ibrutinib-loaded nanobubbles were determined on the 1st, the 10th and the 30th day. The appearance of ibrutinib loaded nanobubbles was also observed using optical microscopy to evaluate the integrity of their structures.

Determination of haemolytic activity [12]

Human blood was used to assess the hemolytic activity of chitosan nanobubbles. As different concentrations of nanobubbles formulations (1, 2, 4, 6, 8 and 10%), were added to a suspension of erythrocytes (30%, v/v) in phosphate buffer at pH 7.4. To obtain the haemolytic control, a suspension of erythrocytes (30%, v/v) in phosphate buffer pH 7.4 was used as the blank condition, to which an excess of ammonium chloride was added to complete haemolysis. During the incubation process, the samples were incubated at 37 degrees Celsius for two hours. Following centrifugation for 10 minutes at 3000 RPM, the supernatants were analyzed using a spectrophotometer with a wavelength of 543 nm. We calculated the percent hemolysis in relation to a control of 100% hemolysis using the following equation.

$$\%\ Hemolysis = \frac{ABS_{Sample} - ABS_0}{ABS_{100} - ABS_0} X\ 100$$

Where ABS_0 and ABS_{100} are the absorbance of the solution at 0 and 100 % hemolysis, respectively.

In vitro cellular uptake study [13]

Cellular uptake of ibrutinib and ibrutinib loaded nanobubbles qualitatively investigated by using confocal laser scanning microscopy. HepG2 cells were put into confocal chamber and were cultivated overnight before they were co-cultivated with free ibrutinib dissolved in DMSO (50 µM), Ibrutinib nanobubbles without sonication (50 µM) and ibrutinib nanobubbles with sonication (50 µM).

At different time intervals, cells were photographed by using confocal laser scanning microscopy under blue filtered glasses at excitation wavelength of 405 nm. These formulations at a dosage of 50 µM were mixed with the cell lines and continuously cultivated for 2 h, respectively. The fluorescent intensity in each plate was determined by fluorescent microplate at excitation wavelength of 503 nm and emission wavelength of 528 nm, respectively. All the trials were performed in triplicate.

In vitro cell cytotoxicity assay [14]

HepG2 cells were incubated in DMEM containing 10% fetal calf serum and then transferred into 96-well plates at a density of 5×10^4 per well at 37 °C under 5% CO_2 atmosphere. The blank, Ibrutinib dissolved in DMSO, Ibrutinib nanobubbles without sonication (50 µM) and ibrutinib nanobubbles with sonication (50 µM) at different concentrations were added into each well with a ratio of cultural medium to non-medium equivalent to 9:1 after incubation to be full throughout the wells, respectively. After incubation for 24 and 48 h, each well was treated with MTT (5 mg/ml) for 4 h, respectively. Then the medium was discarded and to each well dimethyl sulfoxide was added to dissolve formazan at 25 °C. Absorbance was determined at 570 nm in Microplate Absorbance Reader (Model 680; Bio-Rad Laboratories, Hercules, CA).

Statistical analysis

Data are expressed throughout the text as mean ± SD, calculated from at least three different experiments. Statistical analyses were performed using unpaired Student's t-test. Statistical significance was set at $p<0.05$.

RESULTS AND DISCUSSION

A sequence of seventeen trials was executed as per a 3^3 BBD. The obtained results from the randomized trials for the selected independent variables and dependent variables are presented in Table 4.

Several batches of ibrutinib loaded nanobubbles were prepared by varying the conc. of formulation components. Inconsistent particle size distribution was observed from the results of preliminary experiments. It is evident from the preliminary experiments that the concentration(conc.) of L-α-Phosphatidylcholine (A), conc. of chitosan (B) and conc. of palmitic acid (C), had a major impact on the PLS & PI of nanobubbles.

The BBD method was used to optimize the preparation conditions. The selected model was found to be significant in terms of particle size and polydispersity index as designated by the corresponding 'p' values of less than 0.05. The summary of the design is as shown in figure 1.

Study Type	Response Surface	**Runs**	17
Design Type	Box-Behnken	**Blocks**	No Blocks
Design Model	Quadratic	**Build Time (ms)**	45.88

Factor	Name	Units	Type	Subtype	Minimum	Maximum	-1 Actual	+1 Actual	Mean	Std. Dev
A	Concentration of L-alpha phc	w/v	Numeric	Continuous	1.00	2.00	1.00	2.00	1.50	0.34
B	Concentration of chitosan	w/v	Numeric	Continuous	1.00	3.00	1.00	3.00	2.00	0.69
C	Concentration of palmitic aci	w/v	Numeric	Continuous	0.50	1.50	0.50	1.50	1.00	0.34

Response	Name	Units	Obs	Analysis	Minimum	Maximum	Mean	Std. Dev.	Ratio	Trans	Model
Y1	Particle size	nm	17	Polynomial	198.12	416.42	338.617	66.7437	2.10186	None	RQuadratic
Y2	Ploydispersity index		17	Polynomial	0.16	0.51	0.304706	0.095598	3.1875	None	RQuadratic

Figure1: Summary of the BBD

RSM optimization

Statistical analysis

The particle size (Y1) for all the trials was found to be in the range of 198.12-416.42 nm. Similarly, the range of PDI (Y2) was 0.16-0.51. All the results were fitted into a 2^{nd} order quadratic model and the appropriateness of this model was confirmed by ANOVA, lack of fit and multiple regression coefficient (R^2) values. (table 3)

Table 3: Regression equations for the responses

Dependent Variable	Regression equation
Y1	$397.9784 + 2.3175\ A - 36.795\ B - 26.1025\ C + 9.055\ AC - 11.26\ BC - 111.184\ B^2 - 14.9589\ C^2$
Y2	$0.262105 - 0.0025\ A - 0.015\ B - 0.1225\ C + 0.0325\ AC - 0.0175\ BC + 0.040263\ A^2 + 0.050263\ C^2$

Particle size

The PLS of nanobubbles was within 198.12-416.42 nm [15].The polynomial model shown that all the variables (A, B and C) have a significant consequence on PLS of nanobubbles. The interactive effect of A and C (AC) at constant level of B on particle size is as shown in figure 2,3. The interactive effect of B and C (BC) at constant level of A on particle size is as shown in figure 4,5,6.

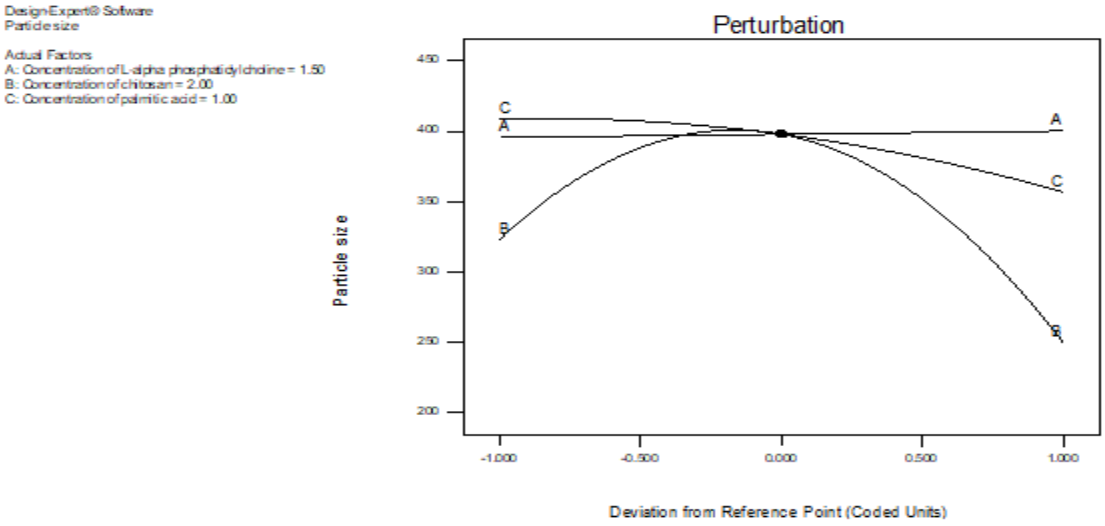

Figure 2: Two dimensional PP– impact of A, B and C on PLS

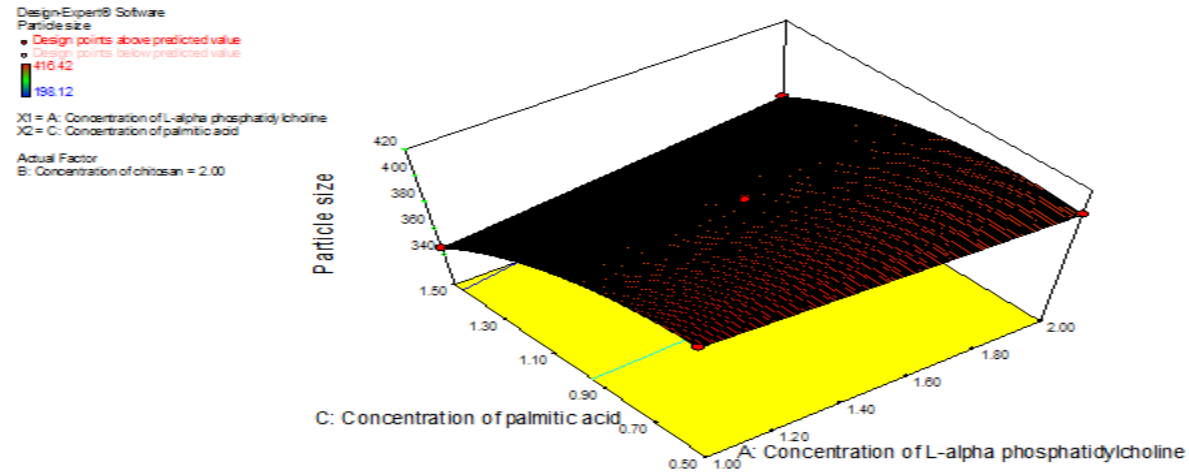

Figure 3: 3D- RSP showcasing the impact of A & C on PLS at constant level of B

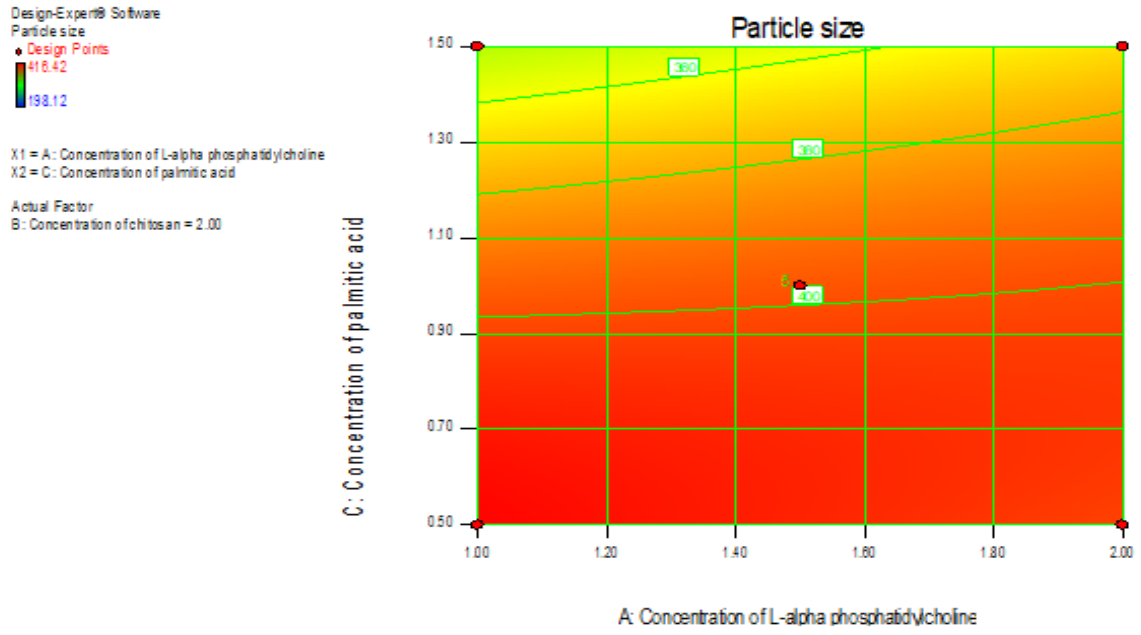

Figure 4: CP showcasing the impact of A and C on PLS at constant level of B

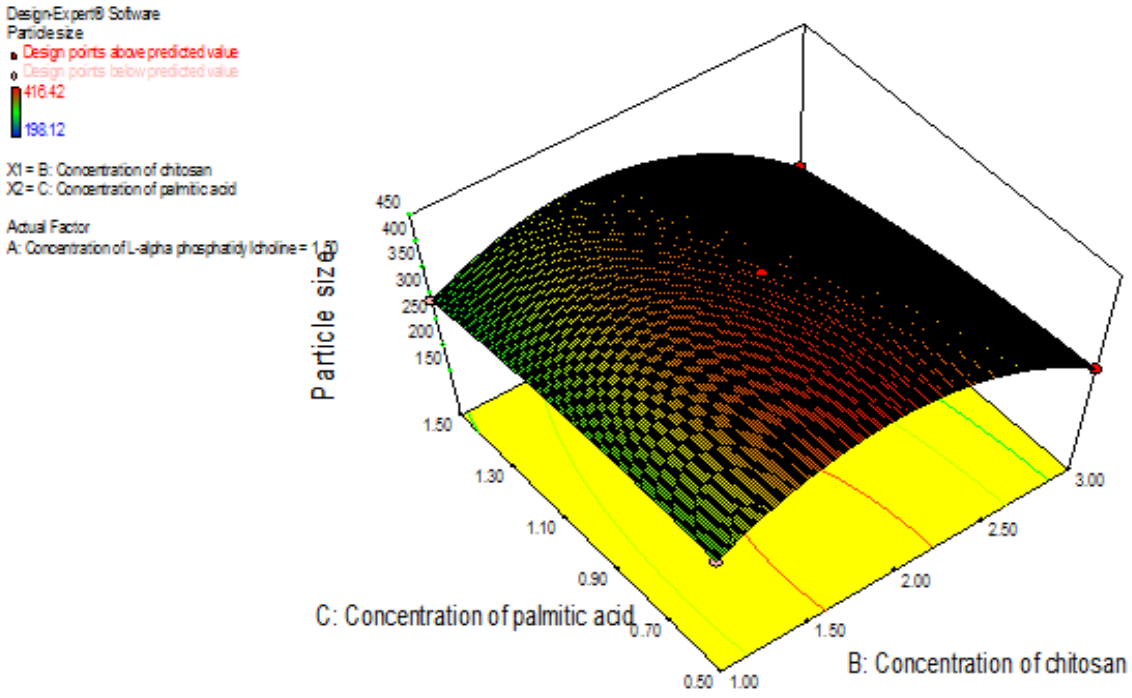

Figure 5:3D- RSP showcasing the impact of B & C on PLS at constant level of A

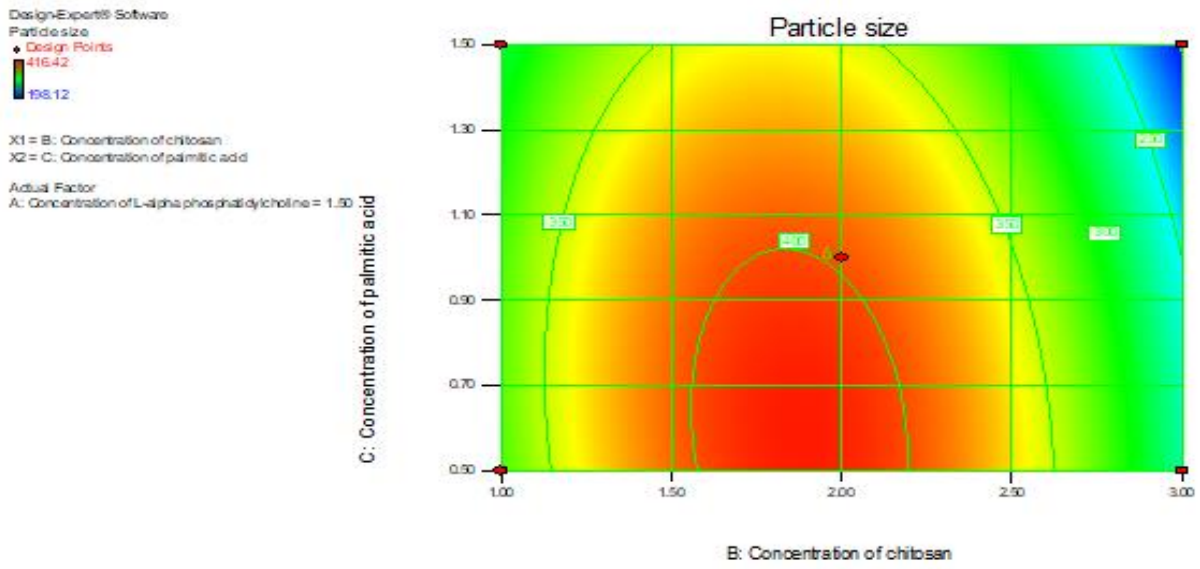

Figure 6: CP showcasing the impact of B & C on PLS at constant level of A

Polydispersity index (Y2)

The PI values of nanobubbles were found to be in the range of 0.16-0.51. The polynomial model shown that all the variables (A, B and C) have a significant effect on the PI of nanobubbles. The observed values are in close agreement with the predicted values.

The 2D and 3D plots clearly indicated that C has major effect on PI followed by B and A have little effect. The interactive effect of A and C (AC) at constant level of B on PI is as shown in figure 7,8. The interactive effect of B &C (BC) at constant level of A on PI is as shown in figure 9,10 and 11.

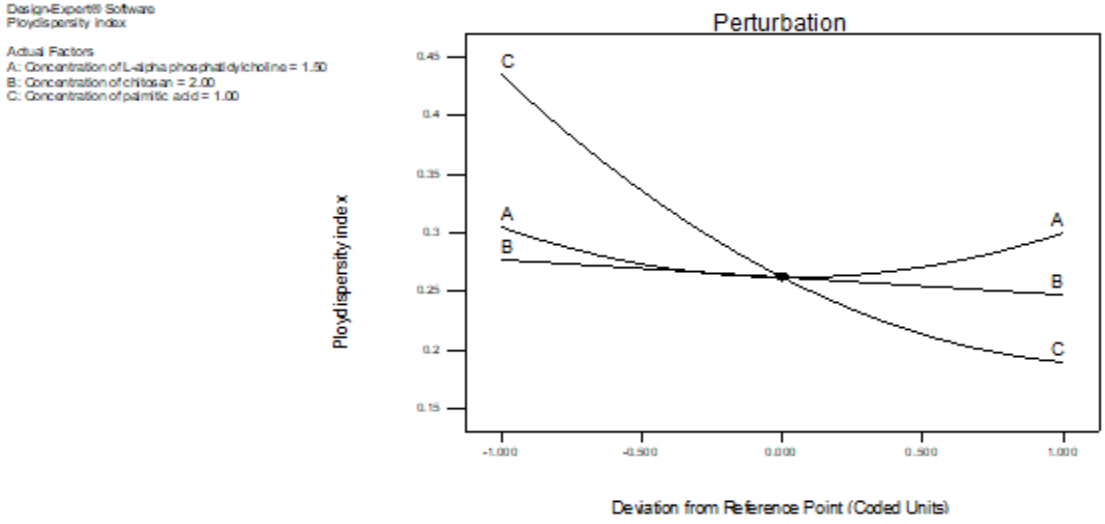

Figure 7: Two dimensional PP– impact of A, B & C on PI

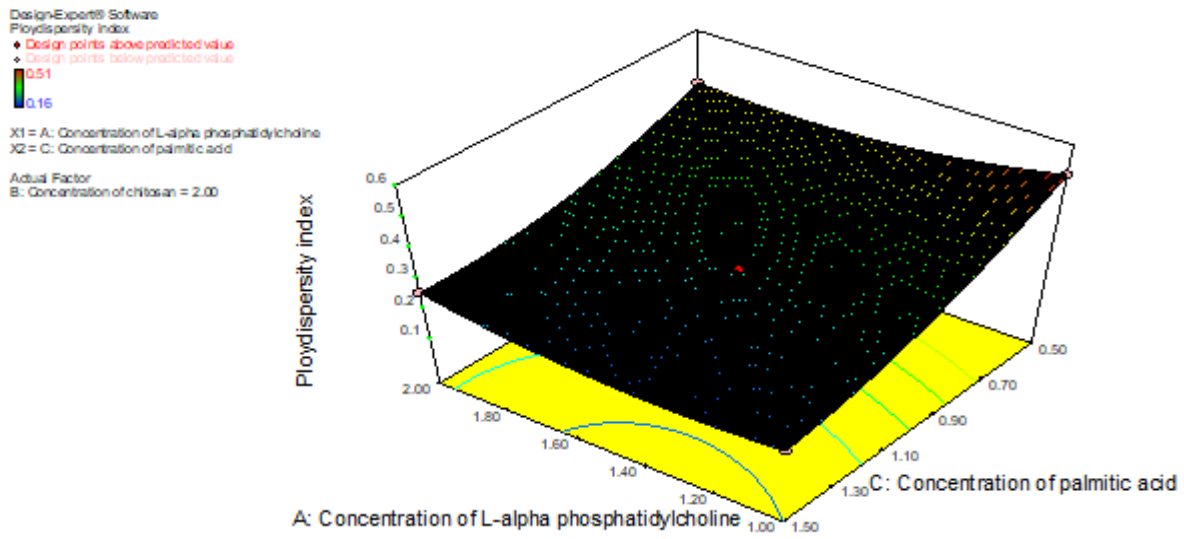

Figure 8: 3D- RSP showcasing the impact of A & C on PI at constant level of B

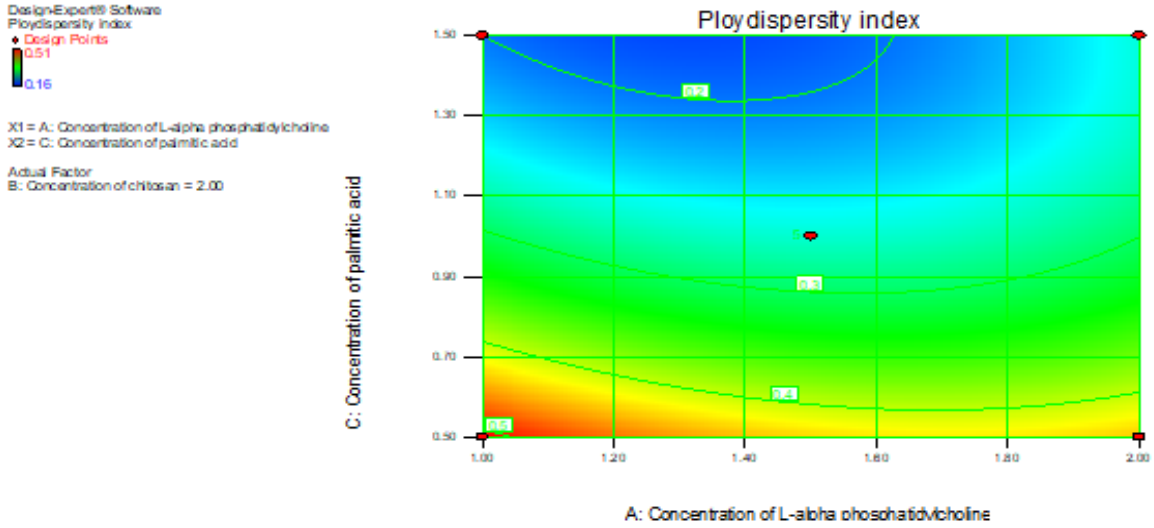

Figure 9: CP showcasing the interactive impact of A &C on PI at constant level of B

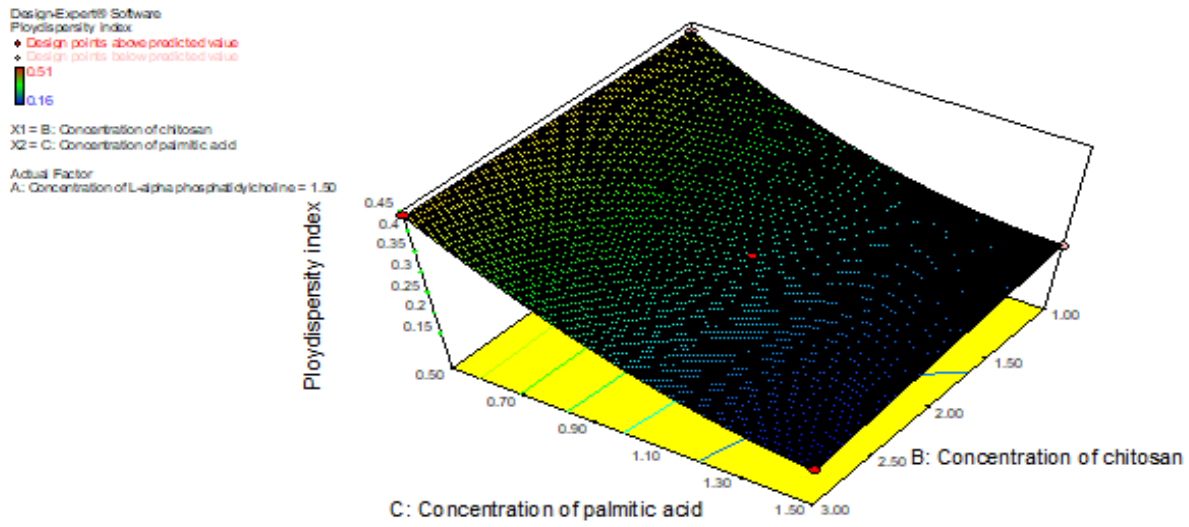

Figure 10:3D- RSP showcasing the impact of B & C on PI at constant level of A

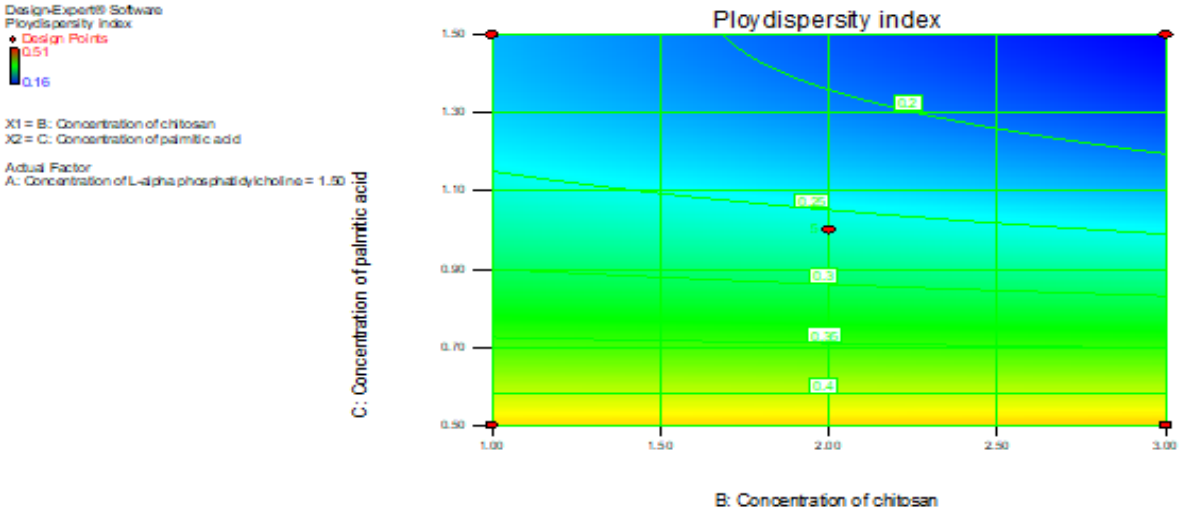

Figure 11: The CP showcasing the interactive impact of B & C on PI at constant level of A

Optimization

Derringer's desirability approach was used to optimize the process variables which influence the response parameters. Both the responses (PLS and PI) were transformed into a desirability scale. Y_{max} and Y_{min} were considered as the objective function (D) for each response. The extreme desirability function value was obtained at A:1.11 % w/v, B:2.95 % w/v, C:1.5 % w/v with the conforming D value of 0.993. To confirm the appropriateness of the model, three executive bathes of nanobubbles were prepared under optimal conditions [16]. The response parameters for the prepared batches are as shown in Table 4. A close accord found among predicted and experimental results, demonstrating the validity of the BBD combined with a derringer's desirability approach for the optimization of ibrutinib nanobubbles.

The PLS of all the batches of ibrutinib nanobubbles was found to be similar with low polydispersity indices. TEM images revealed the superficial morphology and core-shell structure of nanobubbles in the size range of 150-200 nm(figure 12). Moreover, the PLS determined by dynamic light scattering method is correlated well with the TEM measurement.

Table 4: Optimum conditions attained by applying restrictions on response parameters

Independent variables	**Optimized values**	**Predicted values**		**Actual values**			
		PLS (Y1) nm	**PI (Y2)**	**Batch**	**PLS (Y1) nm**	**PI (Y2)**	**ZP (mV)**
Concentration of L-α-Phosphatidylcholine	1.11	201.329	0.15999	B1	198.36 ± 8.34	0.17 ± 0.005	38.34 ± 3.36
Concentration of Chitosan	2.95			B2	206.18 ± 6.28	0.18 ± 0.005	42.88 ± 2.28
Concentration of palmitic acid	1.5			B3	201.66 ± 7.12	0.16 ± 0.005	39.76 ± 1.89

Table 5: Physical characteristics of nanobubbles

	Blank nanobubbles	**Ibrutinib loaded nanobubbles**
Average particle size	199.82 ± 10.12	201.66 ± 7.12
Polydispersity index	0.20 ± 0.005	0.16 ± 0.005
Zeta potential	52.36 ± 2.42	39.76 ± 1.89
Encapsulation efficiency	-	82.58 ± 3.17
Loading capacity	-	17.12 ± 2.66

Nanobubbles were able to load ibrutinib with an encapsulation efficiency of 82.58 % and loading capacity of 17 %. (table 5) The loading of ibrutinib in the nanobubble structure did not significantly affect the viscosity of the formulations.

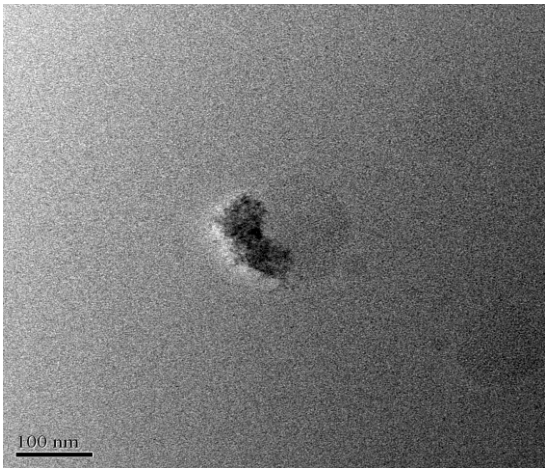

Figure 12. TEM image of ibrutinib nanobubbles

Differential scanning calorimetry thermogram of ibrutinib loaded chitosan nanobubbles are reported in Figure 13. The DSC curve of ibrutinib has shown an endothermic peak at 159.12 °C corresponding to its melting point. The DSC curve of chitosan has shown an endothermic peak at 87.82°C. The DSC curve of blank nanobubbles has shown two endothermic peaks. The first broad peak at about 73.406 °C is related to evaporation of water, while the second peak in the range of 90-100°C is connected to the glass transition temperature of water embedded chitosan matrix. Chitosan nanobubbles showed an endothermic peak at 98.34 °C, while chitosan showed a peak at 87.82°C. The difference in melting temperature indicating the change in the polysaccharide matrix in the nanobubbles structure. The disappearance of characteristic endothermic peak of drug indicating the complete inclusion of the drug within the core structure.

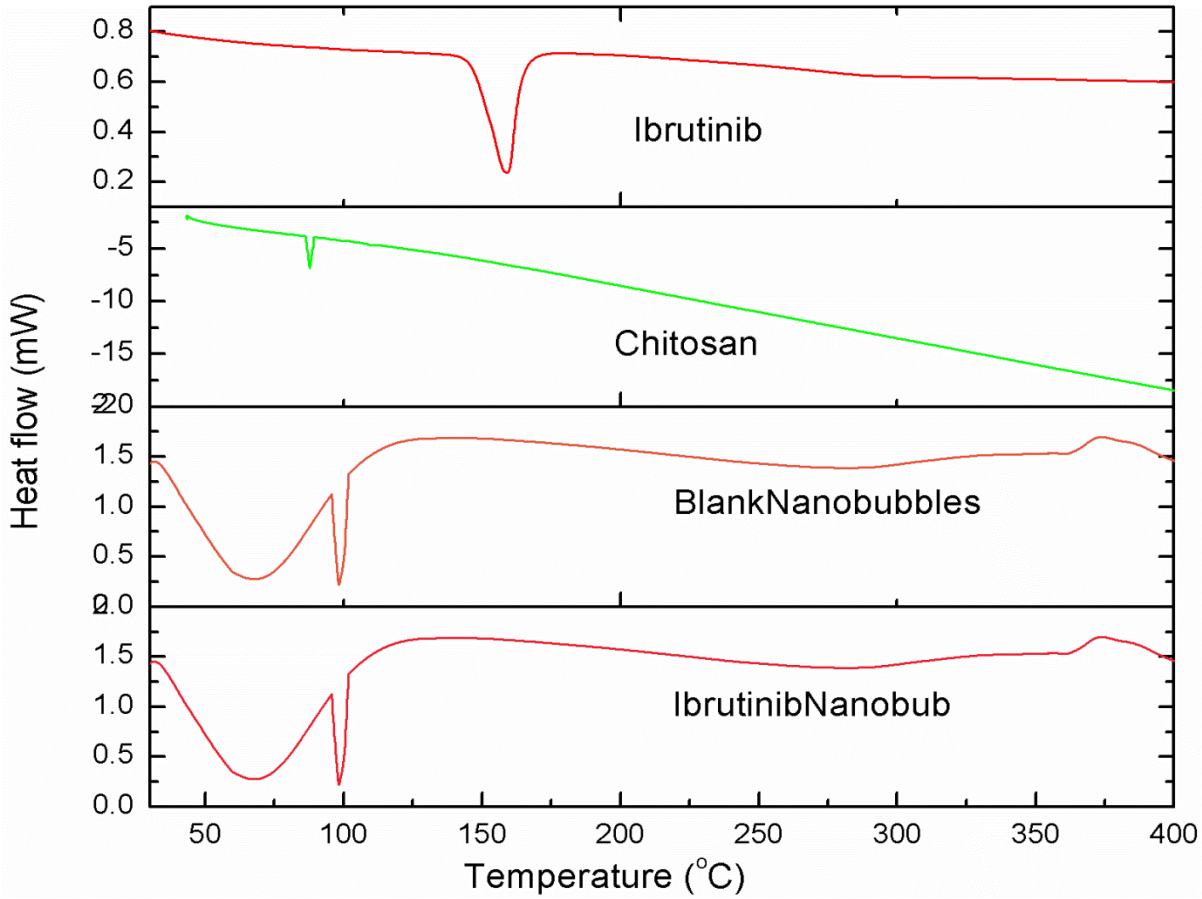

Figure 13. DSC thermogram of ibrutinib, Chitosan, blank nanobubbles and ibrutinib loaded nanobubbles

The amount of drug released from nanobubbles was significantly higher than that from the ibrutinib suspension. Significant difference was observed between the drug released from ultrasound assistance and non-ultrasound assistance. After 6 h, the 48.53 % of ibrutinib was released under sonication, whereas only 18.88 % released without sonication. Without ultrasound only 54.76 % of ibrutinib released after 24 h. In contrast, almost 93.52 % of ibrutinib was released with ultrasound. The results suggested that ultrasound assistance may promote the release of ibrutinib from the nanobubbles due to cavitation effect.(figure 14)

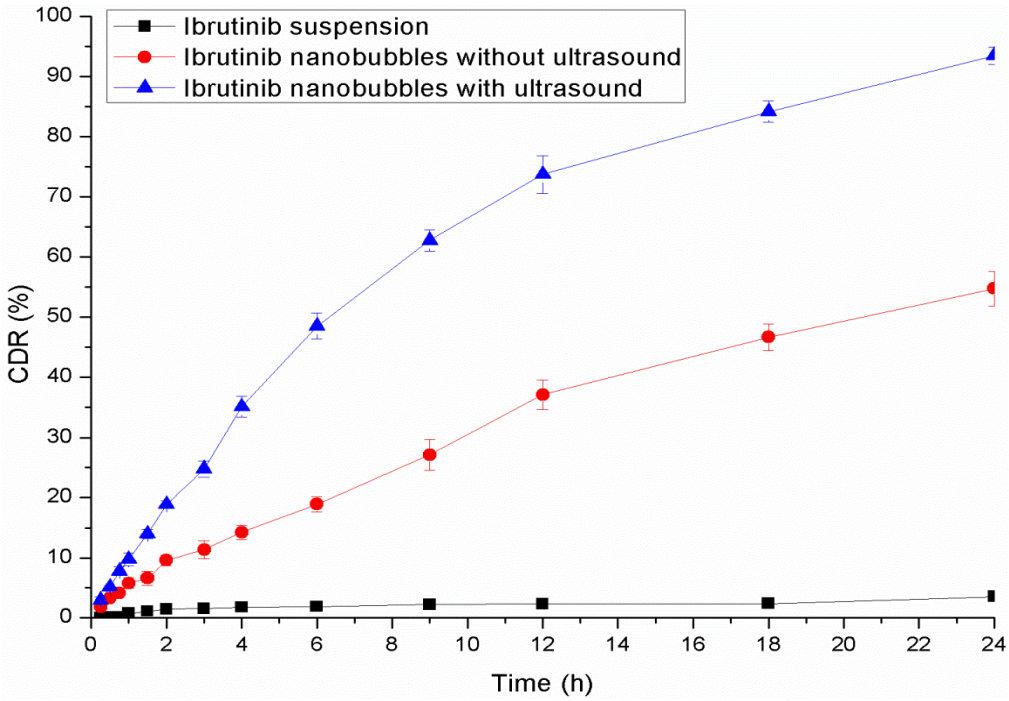

Figure 14. In-vitro drug release pattern with and without ultrasound assistance

The stability of ibrutinib loaded nanobubbles was evaluated after exposure to ultrasound at different temperatures. After 5 minutes of sonication (2.5 MHz) at 25°C, the morphology and structure Nanobubbles remains unaffected. On the contrary, at 37°C, nanobubbles begin to disappear at 3 minutes and completely disappeared after 5 minutes of sonication, indicating the decrease in stability.

The storage stability of ibrutinib nanobubbles was evaluated at different temperatures (4 °C, 25 °C and 40°C) for 1 month.The data on drug content, encapsulation efficiency and particle size of ibrutinib nanobubbles at 0, 15 and 30 days are shown in table 6. No significant change in drug content was observed at lower temperatures. The encapsulation efficiency hardly changed at 4 °C and 25 °C, indicating that nanobubbles could protect ibrutinib from degradation or deterioration at normal temperature. At higher temperature, the encapsulation efficiency significantly reduced, indicating the disruption of nanobubbles structure at higher temperature.

Table 6: Encapsulation efficiency, PLS and PI of ibrutinib nanobubbles stored at different temperatures

Temperature (°C)	Time (days)	Encapsulation efficiency (%)	PLS (nm)	PI
4 ± 1 °C	0	82.58 ± 3.17	201.66± 7.12	0.16± 0.005

	15	81.44± 2.12	198.22 ± 4.88	0.16± 0.005
	30	81.12± 0.96	197.33 ± 3.94	0.17± 0.005
25 ± 2 °C	0	82.58 ± 3.17	201.66 ± 7.12	0.16 ± 0.005
	15	80.12 ± 1.76	196.22 ± 4.88	0.182 ± 0.005
	30	79.88 ± 1.92	195.33 ± 3.94	0.224 ± 0.005
40 ± 2 °C	0	82.58 ± 3.17	201.66 ± 7.12	0.16 ± 0.005
	15	77.72 ± 0.88	248.12 ± 1.84	0.236 ± 0.005
	30	72.12± 2.06	376.34 ± 2.12	0.388 ± 0.005

n = 3 ($p < 0.05$)

The non-toxicity of formulation for parenteral administration is mandatory requirement. Hence to evaluate the safety of the blank nanobubbles and ibrutinib loaded nanobubbles, the hemolytic activity was determined. The aqueous suspensions of chitosan nanobubbles were found to be non-hemolytic up to the tested concentration of 5 mg/ml. Drug loaded nanobubbles also showed a good safety profile with erythrocytes.

In vitro cellular uptake study

The cellular uptake of ibrutinib from nanobubbles formulation in HepG2 cells was determined using fluorescent intensity analysis. The fluorescent intensity data generated from HepG2 cells after incubation for 2 h is presented in figure 15. Cells treated with Ibrutinib Nanobubbles with ultrasound showed mean fluorescence intensity of 6.12 in HepG2 cells, which is 1.5 times higher than that treated with Ibrutinib Nanobubbles without ultrasound. This data indicates the enhanced cellular uptake of ibrutinib with ultrasound from nanobubbles.

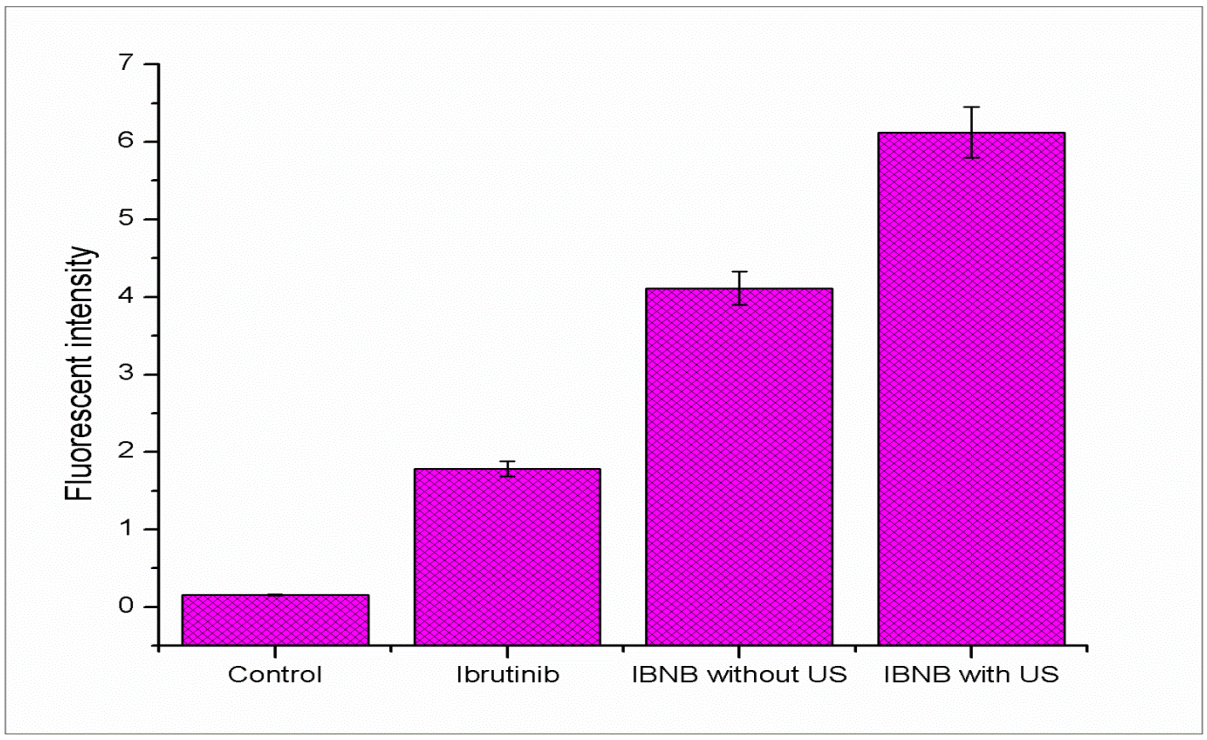

Figure 15: Results of Cellular uptake study

In-vitro cytotoxicity study

In vitro cytotoxicity of ibrutinib loaded nanobubbles against HepG2 cells was performed using MTT assay method (figure 16). HepG2 cells exhibited more than 98 % viability when exposed to capsaicin formulations at lower concentration (10 µM) irrespective of formulation. The cell viability was greater than 83 % even at concentration of ibrutinib at 20 µM, which might be caused by lower concentration than minimum effective concentration. As the concentration increases nanobubbles with ultrasound resulted in the lowest cell viability among all three formulations. The IC50 values of free ibrutinib, IB nanobubbles without ultrasound and IB nanobubbles with ultrasound were 94.2, 81.76 and 70.42 µM. This result indicated that ultrasound assisted nanobubbles can effectively released in the cells with high sensitivity.

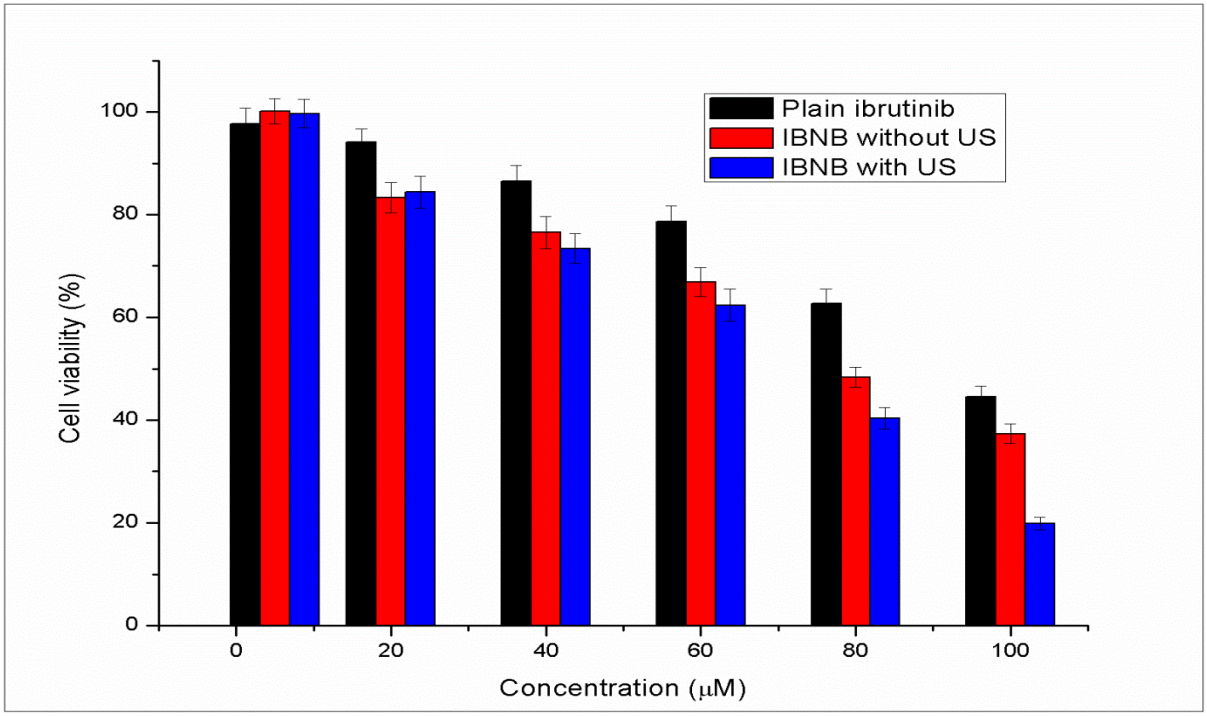

Figure 16: In vitro cytotoxicity of plain ibrutinib, ibrutinib nanobubbles without ultrasound and ibrutinib nanobubbles with ultrasound

CONCLUSION

In this study, chitosan-shelled and perfluropentane filled nanobubbles were developed for the delivery of anticancer drug ibrutinib. The formulation components were optimized with respect to particle size and size distribution using response surface methodology. Nanobubbles prepared under optimal conditions exhibited uniform particle size distribution. Compared with the solubility of ibrutinib suspension, that of the ibrutinib nanobubbles is significantly increased at different pH values. In vitro dissolution test demonstrated that compared with the suspension, ibrutinib nanobubbles displays better dissolution profiles and higher gastrointestinal stability, leading to a significant increase in oral bioavailability. Moreover, in vitro cytotoxicity studies illustrated that ibrutinib nanobubbles displayed superior growth inhibition of tumor cells.

CONFLICT OF INTEREST

I do not declare any relationships (conflict of interests) that could affect the objectivity and credibility of present work.

FUNDING SOURCES

Self-financed

REFERENCES

1. Kanamala M, Wilson WR, Yang M, Palmer BD, Wu Z. Mechanisms and biomaterials in pH-responsive tumour targeted drug delivery: a review. Biomaterials. 2016;85:152-67.
2. Chen EM, Quijano AR, Seo YE, Jackson C, Josowitz AD, Noorbakhsh S, Merlettini A, Sundaram RK, Focarete ML, Jiang Z, Bindra RS. Biodegradable PEG-poly (ω-pentadecalactone-co-p-dioxanone) nanoparticles for enhanced and sustained drug delivery to treat brain tumors. Biomaterials. 2018; 178:193-203.
3. Zhang C, Cao H, Li Q et al. Enhancement effect of ultrasound-induced microbubble cavitation on branched polyethylenimine-mediated VEGF165 transfection with varied N/P ratio. Ultrasound Med Biol. 2013;39:161–171.
4. Van LA, Knoop RJ, Kappen FH, Boeriu CG. Chitosan films and blends for packaging material. CarbohydrPolym. 2015; 116:237–242.
5. Nazzal S, Khan MA. Response surface methodology for the optimization of ubiquinone self-nanoemulsified drug delivery system. AAPS Pharmscitech. 2002;3(1):23-31.
6. Cavalli R, Bisazza A, Giustetto P, Civra A. Preparation and characterization of dextran nanobubbles for oxygen delivery. Int J Pharm. 2009; 381(2): 160–165.
7. Abdullah S, Mohammad J, Anwer, Majid A. Enhanced Oral Bioavailability of Ibrutinib Encapsulated Poly (Lactic-co-Glycolic Acid) Nanoparticles: Pharmacokinetic Evaluation in Rats. CurrPharmac Anal. 2019;15: 661-668.
8. Cavalli, Roberta &Bisazza, Agnese&Trotta, Michele &Argenziano, Monica &Civra, Andrea &Donalisio, Manuela &Lembo, David. New chitosan nanobubbles for ultrasound-mediated gene delivery: Preparation and in vitro characterization. Int journal of nanomed. 2012;7:3309-18.
9. Abenojar EC, Nittayacharn P, De Leon A, Perera R. Effect of Bubble Concentration on the in Vitro and in Vivo Performance of Highly Stable Lipid Shell-Stabilized Micro- and Nanoscale Ultrasound Contrast Agents. Langmuir. 2019; 35:10192.
10. Hernandez C, Abenojar E, Hadley J, De Leon AC, Coyne R. Perera R. Sink or Float? Characterization of Shell-Stabilized Bulk Nanobubbles Using a Resonant Mass Measurement Technique. Nanoscale 2019; 11: 851– 855.
11. Zhou L, Wang S, Zhang L, Hu J. Generation and stability of bulk nanobubbles: A review and perspective. Current Opinion in Colloid & Interface Science.2020;53:101439.
12. Takano S, Kondo H. Quantitative method for determination of haemolytic activity of Clostridium septicum toxin. Jpn J Med Sci Biol. 1987;40(2):47-59.
13. Zhang Y, Liu AT, Cornejo YR, Van Haute D, Berlin JM. A Systematic comparison of in vitro cell uptake and in vivo biodistribution for three classes of gold nanoparticles with saturated PEG coatings. PLoS One. 2020;15(7): e0234916.
14. Cho MH, Niles A, Huang R, Inglese J, Austin CP, Riss T. A bioluminescent cytotoxicity assay for assessment of membrane integrity using a proteolytic biomarker. ToxicolIn Vitro. 2008; 22(4):1099-106.
15. Kishore Babu, A, Bhanu Teja, B., Ramakrishna, B, Balagangadhar, B, Vijay Kumar, V., Venkat Reddy,V. Formulation and Evaluation of Double Walled Microspheres Loaded with Pantoprazole, IJRPC. 2011; 1(4): 770-779.
16. Mamatha P, Arun Kumar J, Bhikshapathi D. V. R. N. Design and Optimization of Ibrutinib Solid Lipid Nanoparticles Using Design of Experiment, IJBPAS. 2021;10(9): 723-737